

Neural network estimation of a photovoltaic system based on the MPPT controller



Marwa Ben Slimene *, Abdulaziz Aljaloud

Department of Computer Science and Engineering, College of Computer Science and Engineering, University of Hail, Hail, Saudi Arabia

ARTICLE INFO

Article history:

Received 8 September 2019

Received in revised form

16 December 2019

Accepted 19 December 2019

Keywords:

Neural network

Solar radiation sensor

Photovoltaic system

MPPT controller

ABSTRACT

MPPT is necessary to achieve an optimal exploitation of the photovoltaic (PV) system. This paper deals with the problem of the optimization of the power, delivered by the photovoltaic panel (PVP). To achieve this aim, a neural network estimator (NNE), followed by a conversion coefficient and a calculation stage of the optimal duty cycle, has been developed. The NNE is used to calculate the open circuit voltage corresponding to each solar radiation and to a various value of temperature, based only on the standard open circuit voltage. A coefficient, determining for each solar radiation the voltage of the maximum power directly from the open circuit voltage, is estimated by a practical test. Finally, the optimal duty cycle is, next, determined by the input/output equation of the boost converter. The proposed MPPT is tested and compared with the most widely used MPPT methods by simulations using MATLAB/Simulink and real time hardware in the loop (HIL) implementation. The results obtained with the proposed MPPT show excellent dynamic performance under fast irradiation changes.

© 2020 The Authors. Published by IASE. This is an open access article under the CC BY-NC-ND license (<http://creativecommons.org/licenses/by-nc-nd/4.0/>).

1. Introduction

Amongst all renewable energy sources, solar energy provides an excellent opportunity for the production of electricity and therefore this energy is widely used. Solar energy is a clean renewable resource with zero emission. Due to an increase in power demand, the switch over to renewable energy sources which are eco-friendly and exist abundant in nature is extremely necessary. The efficiency of the PV system is improved by using the maximum power point tracking (MPPT) controller. Frequently used MPPT algorithms are Perturb and Observe (P&O) and Incremental Conductance (INC). In the incremental conductance algorithm, the gradient of the P-V curve is estimated ([Bouselham et al., 2017](#); [Chatrenour et al., 2017](#)).

To date, numerous MPPT controllers have been presented and implemented in the literature, these controllers have some generic requirements such as low complexity, low cost, minimum output power fluctuation, and the ability to track quickly when

operating condition changes. The most widely used algorithms are perturbing and observe (P&O) ([Chatrenour et al., 2017](#); [Ezinwanne et al., 2017](#)) and incremental conductance (InC) ([Jiang et al., 2017](#)). These conventional methods achieve moderate performance with easy implementation and a low cost. For better transient and steady-state performance, artificial intelligence based MPPT techniques have been suggested such as fuzzy logic ([Kwan and Wu, 2017](#)) and neural networks controller (NNC). However, the NNC controller has proved good performance under rapidly varying irradiance, especially in terms of efficiency and response time.

The performances and the anomalies related to several stage inverter architectures used for the prevalent MPPT techniques have been investigated in [Murtaza et al. \(2017\)](#). A new hybrid MPPT algorithm has been proposed to quickly track the MPP of the PV arrays. The algorithm has been implemented in a single-phase two-stage PV inverter in which the direct current sensors for tracking the MPP are not required.

To improve the dynamic response of boost DC-DC converter-based PV system under the sudden insolation and temperature change, a novel fuzzy logic MPPT controller has been proposed in [Rahmani et al. \(2015\)](#) and [Rezk et al. \(2017\)](#), for tracking of MPP.

* Corresponding Author.

Email Address: benslimene.marwa@gmail.com (M. B. Slimene)

<https://doi.org/10.21833/ijaas.2020.02.012>

Corresponding author's ORCID profile:

<https://orcid.org/0000-0002-7660-2337>

2313-626X/© 2020 The Authors. Published by IASE.

This is an open access article under the CC BY-NC-ND license

(<http://creativecommons.org/licenses/by-nc-nd/4.0/>)

Based on the relation between the variation of the open circuit voltage (V_{oc}) and the short-circuit current (I_{sc}) along with the perturb and observe (P&O) techniques, an MPPT technique has been proposed in Khlifi (2016) and Bouselham et al. (2015). The proposed MPPT technique constitutes a control structure that contains three loops. These loops are referred to as the E-MPP loop, R-MPP loop and S-loop. These loops are based on these three considerations (i) the voltage and the current relations of PV that gives MPP, (ii) the duty cycle of the converter to set a PV operating point at MPP, (iii) a criterion to measure the varying weather conditions and the limits criteria to evaluate the steady weather conditions.

In order to improve the response time of NNC to track PV system and reduce the complexity of the controller, this paper proposes a novel MPPT, it consists of a simple algorithm that scans the P-V curve to identify the PV system, combined to NNC which gives the duty cycle corresponding to the DC-DC converter. The remainder of the paper is organized as follows: A description of the considered PV model and its characteristics are introduced in Section 2; while section 3 describes the proposed MPPT method. Section 4 briefs the results and discussions. Finally, conclusions are reported in Section 5.

2. Photovoltaic system model

A novel MPPT controller strategy, coupled with real time accurate estimate of the optimum duty cycle to operate the PVP at its maximum power through a dc-dc converter, has been evolved with the following objectives.

Fig. 1 shows a block diagram of the proposed PV system consisting of the following components: PV Panel, Boost converter, MPPT controller, DC Load.

Fig. 2 shows the power converter stage, that connects the PVP module to the dc load. The power converter stage consists of a boost DC-DC converter to integrate the output filter and the MPPT control unit. The control system detects a maximum power point (P_{max}) of PV systems. The MPPT drives the operating point of the PVP to the P_{max} .

The control unit optimizes the duty cycle, in real time, to control the boost converter and make the PVP operate in its maximum power for varying insolation. With steady state operation, the transfer function for boost converter is deduced as follows:

$$V_L = \frac{V_{PV}}{1-\alpha} \quad (1)$$

where α is the duty cycle of boost DC-DC converter evaluated by the control unit, V_L is the boost DC-DC converter output voltage and V_{PV} is the output voltage of PVP.

Fig. 2 represents the equivalent electrical circuit of the PV cell as a current source in parallel with a diode.

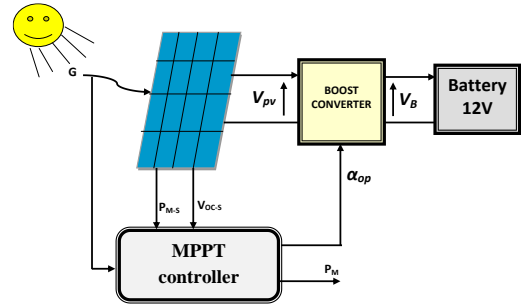


Fig. 1: PV system with MPPT controller

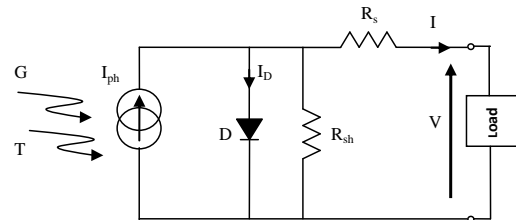


Fig. 2: Equivalent electrical circuit of PV cell

According to Fig. 2, the relationship between the current and the voltage in a single diode is expressed as follows:

$$I = I_{ph} - I_s \left[\exp \left(\frac{q(V - IR_s)}{KTA} \right) - 1 - \frac{V + IR_s}{R} \right] \quad (2)$$

The photocurrent I_{ph} is given by the Eq. 3:

$$I_{ph} = \frac{G}{G_{ref}} [I_{phref} + C_t(T - T_r)] \quad (3)$$

where G is the insolation and T is the cell temperature in Kelvin.

The reverse saturation current (I_{rs}) of the PV cell is dependent on the PV cell temperature T and expressed as follows:

$$I_s = I_{sref} \left[\frac{T}{T_{ref}} \right]^3 \exp \left(\frac{qEg}{KA} \left[\frac{1}{T_{ref}} - \frac{1}{T} \right] \right) \quad (4)$$

To form an array these PV cells are connected in series and parallel. In an array, all PV cells are considered to have the same characteristics. The equivalent circuit of the PV array is presented in Fig. 3.

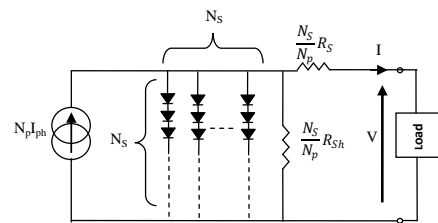


Fig. 3: Single diode model of a PV array

From Fig. 5, the voltage-current relationship of the PV array is as follows:

$$I = N_p I_{ph} - N_p I_s \left[\exp \left(\frac{q(V - IR_s)}{KTA} \right) - 1 - \frac{V + IR_s}{R} \right] \quad (5)$$

The model parameters of the PV system are specified in Table 1.

The problem associated with MPPT techniques is to find the operating condition, i.e. current I_{MPP} and corresponding voltage V_{MPP} , for a PV array to acquire the maximum power output P_{MPP} under given insolation.

Most approaches are pertinent to the variations in both, the PV cell temperature and the irradiance. However, some of the techniques are explicitly more suitable if the PV cell temperature remains roughly constant. In this case, the Perturb and Observe (P&O) are used as the MPPT Control Algorithm. To implement the Control Algorithm, the array must certainly be coupled with a power converter that can vary the current delivered by the PV array.

2.1. Boost converter

A power converter has been interleaved between the PV generator and the load to enhance the performance of a PV system. The DC-DC boost converter is shown in Fig. 4. This converter delivers the appropriate voltage to the load by controlling the duty cycle α . The MPPT tracking algorithm evaluates the MPP operating point of the PVP under varying insolation and PV cell temperature. Thereafter duty cycle α has been estimated corresponding to evaluated MPP.

Table 1: The electrical parametric characteristics of the 50w single-crystalline PV module SM50-H [19]

Parameter (AT STC)	Abbreviation	Value
Band-gap energy	Eg	1.12eV
Ideal factor	A	1.33
Maximum power	Pmax	4.9 wp
Rated current	Impp	0.68 A
Rated voltage	Vmpp	8.1 A
Short circuit current	Isc	0.79A
Open circuit voltage	Voc	12V
Cell modules	Ns	33
Temperature	Ki	1.2Ma/C

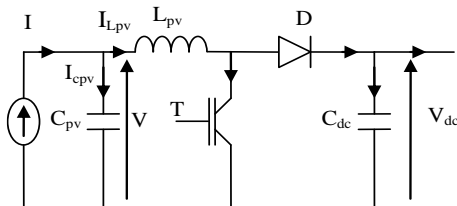


Fig. 4: Equivalent electrical circuit for DC-DC Boost converter

Eq. 6 represents the dynamic model for the dc-dc boost converter.

$$\begin{cases} \frac{dV}{dt} = \frac{1}{C_{pv}}(I - I_{pv}) \\ \frac{dL}{dt} = \frac{1}{L_{pv}}(V - (1 - \alpha_{pv})V_{dc}) \end{cases} \quad (6)$$

2.2. The proposed MPPT method

To operate the PVP in its maximum power mode for varying insolation and PV cell temperature the MPPT control constitutes two stages. The first stage evaluates the maximum power delivered by the photovoltaic panel (PVP). The second stage

estimates the optimal duty cycle to control the boost converter.

2.2.1. Estimation of maximum power

Eq. 7 has been deduced to estimate the maximum power drawn by the PVP for varying solar radiation. This equation needs just the standard maximum power given by the builder at the back of the PVP (PM at 25°C and 1000W/m²). To estimate in real time, the maximum power P_M for varying solar radiation changes, in real time, all day.

$$P_M = P_{M-s} \frac{G}{1000} \quad (7)$$

2.2.2. Neural network estimator

An Artificial Neural Network (ANN) estimator is used in the presented study as shown in Fig. 5. It illustrates the used strategy to estimate the optimal duty cycle, α_{op} , for varying solar radiation values, in real time.

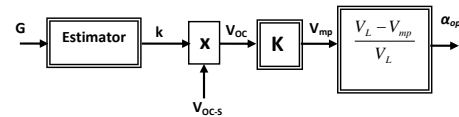


Fig. 5: Optimum duty cycle estimation diagram

The proposed strategy consists in developing an ANN estimator, which is capable to estimate the experimental ratio y . Experimental ratio y is defined as the ratio of open circuit voltage, V_{oc} and the standard open circuit voltage, V_{oc-s} for any solar radiation values G .

$$y = \frac{V_{oc}}{V_{oc-s}} \quad (8)$$

The relation between the output $y(k)$ and the input $G(k)$ is a nonlinear system. It can be expressed by a Nonlinear Auto-Regressive Moving Average (NARMA) model, that is given by the following form:

$$y(k+1) = f[y(k) \dots y(k-ny+1), G(k) \dots] \quad (9)$$

where $f(\cdot)$ is a non-linear function, $y(k) \in \mathbb{R}$ and $G(k) \in \mathbb{R}$ are the outputs and the inputs of the system respectively, k is the discrete time index. ny and nG are the number of the previous samples (data history), of the output and input respectively, required for the prediction.

The system given by the Eq. 9 can be modeled by the neural network approach. The used ANN, in this paper, is a 3-layer feed forward network with perceptron as its element. Input to the ANN is from Tapped delay lines (TDL) from the input and the output of the system. TDL constitutes the delay elements that produces the past samples and presents it as input and output delayed signals. ANN estimator structure for the nonlinear system was shown in Fig. 6.

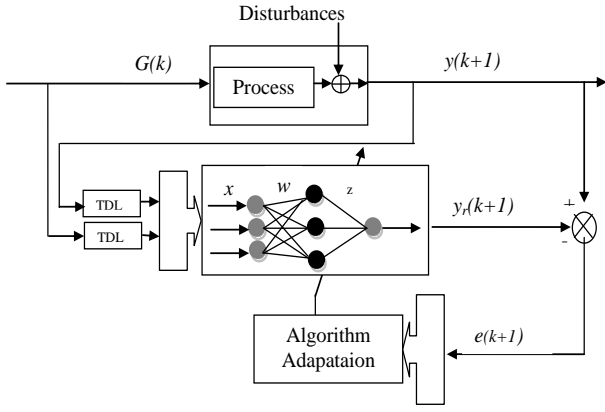


Fig. 6: ANN estimator structure for nonlinear system

These delayed signals are then fed to a static network as the repressor vector so that the predicted neural network output will follow the target output as presented in Fig. 6. Eq. 10 represents the estimated experimental ratio using ANN $y_r(k)$,

$$y(k+1) = \lambda s \left(\sum_{i=1}^{N_1} s \left(\sum_{j=1}^{N_0} w_{ij} x_j \right) \right) z_i = \lambda s \sum_{i=1}^{N_1} s(\text{net}_i) z_i \quad (10)$$

with λ is a regularization coefficient, s is a sigmoid function, w_{ij} and z_i are respectively the hidden synaptic weights and the output synaptic weights, N_0 is the number of neurons in the input layer and N_1 is the number of neurons in the hidden layer. x_j is the input vector of the neural network,

$$x = [G(k), \dots, G(k - n_G), y(k-1), \dots, y(k - n_y)]^T, \\ \text{net}_i = \sum_{j=1}^{N_0} w_{ij} x_j(k),$$

Eq. 11 is the matrix form of (10),

$$y_r(k+1) = \lambda s [Z^T S(Wx)] \quad (11)$$

with,

$$Z = [z_i]_{i=1, \dots, N_1}^T, \\ W = [w_{ij}]_{i=1, \dots, N_1, j=1, \dots, N_0}, \\ S(Wx) = [s(\text{net}_i)]_{i=1, \dots, N_1}^T,$$

$S(Wx)$ is the Jacobian matrix of $S(Wx)$, its derivative is $S'(Wx) = \text{diag}[s'(\text{net}_1), \dots, s'(\text{net}_{N_1})]$.

Using the gradient descent method, given as follows,

$$J(k) = \frac{1}{2} (e(k))^2 = \frac{1}{2} (y_r(k) - y(k))^2 \quad (12)$$

the update for the weights of the output layer of ANN estimator is,

$$z_i(k+1) = z_i(k) - \eta \frac{\partial J(k)}{\partial z_i(k)} \quad (13)$$

$$z_i(k+1) = z_i(k) + \eta \lambda s'(\text{net}_i) S(Wx) e(k) \quad (14)$$

and the update for the weights of the hidden layer of ANN estimator is,

$$w_{ij}(k+1) = w_{ij}(k) - \eta \frac{\partial J(k)}{\partial w_{ij}(k)} \quad (15)$$

$$w_{ij}(k+1) = w_{ij}(k) + \eta \lambda s'(\text{net}_i) S'(Wx) z_i x^T e(k) \quad (16)$$

In Eqs. 13-16, η is the fixed learning rate, $0 \leq \eta \leq 1$. Universal approximator property of the ANN is utilized in the presented work. An ANN has gone under the learning process to learn nonlinear behavior of the process and act as an estimator.

2.2.3. Estimation of optimum duty cycle

The estimated experimental ratio is multiplied by the standard open circuit voltage (given by the builder at the back of the PVP) to give the value of the open circuit voltage for varying solar radiation values G .

Then, a new relationship between the voltage of the open circuit and the corresponding maximum power point voltage, V_{mp} for varying solar radiation, has been established. This relationship has been found, on the basis of the practical experiments as shown in Fig. 7.

Finally, the optimal duty cycle has been calculated directly from the voltage corresponding to the maximum power by the relation of the boost converter.

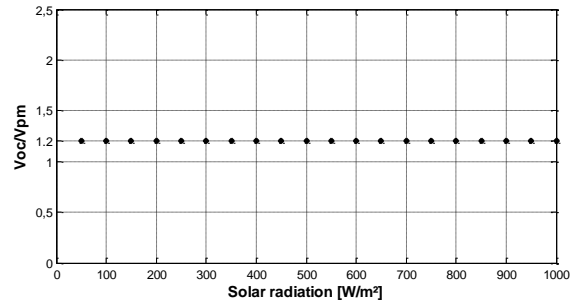


Fig. 7: The relationship of the coefficient V_{oc}/V_{pm} and the solar radiation

$$V_L = \frac{V_{mp}}{1 - \alpha_{op}} \quad (17)$$

The proposed neural network is applied, in the next section, on the photovoltaic supplying system.

3. Simulation results and discussion

Based on the system presented in Fig. 1 and MPPT controller methods, the photovoltaic supply system with DC load (Battery of 24V) has been modeled and simulated in a friendly-user MATLAB/Simulink environment.

In order to check the MPPT performance under the different climatic conditions, real time simulation studies have been performed with real solar radiation.

The ANN estimator has been learned with the learning rate $\eta = 0.42$, the regularization coefficient

$\lambda = 1$, the hidden neurons are 25, the output neuron is equal to 1 and the input vector is,

$$x = [G(k), G(k-1), G(k-2), y(k-1), y(k-2), y(k-3)]^T$$

To prove the efficiency of the ANN estimator a comparison between the real and the estimated values of the experimental ratio of the open circuit for different solar radiation at specified PVP temperatures has been shown in Fig. 8. It gives an almost superposition of the actual and the estimated values of the experimental ratio of the open circuit voltage for different solar radiation at specified PVP temperatures.

We notice that the real and the estimated curves are closely overlapping in the range $400 < G < 1000$, which shows the effectiveness of the neural network estimator to give a value close to the reality, and this gives us the confidence to use this type of estimator in this application. The neural estimator values follow suitably the real one. The error is estimated to be less than 2%.

On the basis of the elaborated relationship between the maximum power point voltage and the open circuit voltage of the PVP, estimated and the real values of the maximum power voltage for the different solar radiation at specified PVP temperature are presented in Fig. 8. The estimated and the real values are proved to be almost conformed to a normalized error of less than 2%.

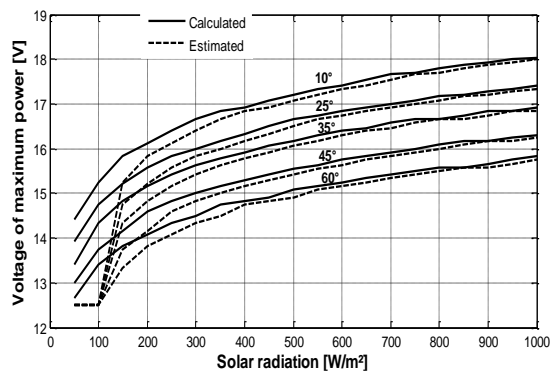


Fig. 8: The real and the estimated values of the maximum power voltage compared by the solar radiation

This clearly demonstrates the effectiveness of MPPT's in properly estimating the optimum value of the duty cycle in real time. The error between the real and the estimated values is around 1%.

Fig. 9 shows the power of the PVP as a function of the voltage as well as the actual and the estimated values of the maximum powers for the different solar radiation values at specified PVP temperature. This curve shows that the estimated values of the maximum power follow the calculated values.

It can be seen in Fig. 9 that the influence of the temperature on the maximum power of the photovoltaic panel is remarkable with the increasing value of solar radiation.

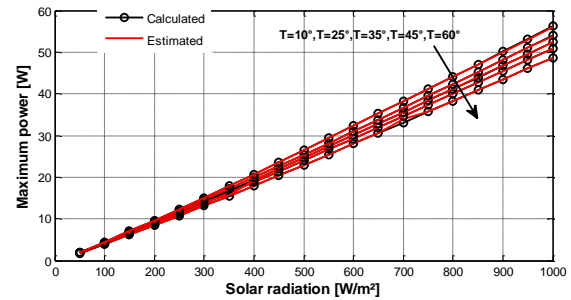


Fig. 9: Variation of maximum power in function of solar radiation

4. Conclusion

In this paper, an intelligent MPPT method has been proposed to track the PV system under different weather conditions for standalone PV systems. The method consists in the development of the neural network estimator, which is able to determine, in real time, at various values of temperature, the value of the open circuit voltage due to any solar radiation value. The simulation results demonstrate that the proposed method guarantees a rapid convergence to the MPPT with good efficiency. The results have shown that the three methods are able to track the MPPT but the proposed method provides better results in terms of response time.

Compliance with ethical standards

Conflict of interest

The authors declare that they have no conflict of interest.

References

- Bouselham L, Hajji B, and Hajji H (2015). Comparative study of different MPPT methods for photovoltaic system. In the 3rd International Renewable and Sustainable Energy Conference (IRSEC), IEEE, Marrakech, Morocco: 1-5. <https://doi.org/10.1109/IRSEC.2015.7455085>
- Chatrenour N, Razmi H, and Doagou-Mojarrad H (2017). Improved double integral sliding mode MPPT controller based parameter estimation for a stand-alone photovoltaic system. *Energy Conversion and Management*, 139: 97-109. <https://doi.org/10.1016/j.enconman.2017.02.055>
- Jiang JA, Su YL, Kuo KC, Wang CH, Liao MS, Wang JC, and Shieh JC (2017). On a hybrid MPPT control scheme to improve energy harvesting performance of traditional two-stage inverters used in photovoltaic systems. *Renewable and Sustainable Energy Reviews*, 69: 1113-1128. <https://doi.org/10.1016/j.rser.2016.09.112>
- Khelifi MA (2016). Study and control of photovoltaic water pumping system. *Journal of Electrical Engineering and Technology*, 11(1): 117-124. <https://doi.org/10.5370/JEET.2016.11.1.117>
- Kwan TH and Wu X (2017). The lock-on mechanism MPPT algorithm as applied to the hybrid photovoltaic cell and thermoelectric generator system. *Applied Energy*, 204: 873-886. <https://doi.org/10.1016/j.apenergy.2017.03.036>
- Loubna Bouselham L, Hajji M, Hajji B, and Bouali H (2017). A new MPPT-based ANN for photovoltaic system under partial

- shading conditions. Energy Procedia, 111: 924-933.
<https://doi.org/10.1016/j.egypro.2017.03.255>
- Murtaza AF, Chiaberge M, Spertino F, Shami UT, Boero D, and De Giuseppe M (2017). MPPT technique based on improved evaluation of photovoltaic parameters for uniformly irradiated photovoltaic array. Electric Power Systems Research, 145: 248-263.
<https://doi.org/10.1016/j.epsr.2016.12.030>
- Osioma Ezinwanne O, Zhongwen F, and Zhijun L (2017). Energy performance and cost comparison of MPPT techniques for photovoltaics and other applications. Energy Procedia, 107: 297-303.
<https://doi.org/10.1016/j.egypro.2016.12.156>
- Rahmani B, Li W, and Liu G (2015). An advanced universal power quality conditioning system and MPPT method for grid integration of photovoltaic systems. International Journal of Electrical Power and Energy Systems, 69: 76-84.
<https://doi.org/10.1016/j.ijepes.2014.12.031>
- Rezk H, Fathy A, and Abdelaziz AY (2017). A comparison of different global MPPT techniques based on meta-heuristic algorithms for photovoltaic system subjected to partial shading conditions. Renewable and Sustainable Energy Reviews, 74: 377-386.
<https://doi.org/10.1016/j.rser.2017.02.051>